ACS APPLIED MATERIALS & INTERFACES

RESEARCH ARTICLE

www.acsami.org

Colored and Functional Silver Nanoparticle–Wool Fiber Composites

Fern M. Kelly and James H. Johnston*

School of Chemical and Physical Sciences and the MacDiarmid Institute for Advanced Materials and Nanotechnology, Victoria University of Wellington, P.O. Box 600, Wellington, New Zealand

ABSTRACT: Silver nanoparticles utilizing the surface plasmon resonance effect of silver have been used to color merino wool fibers as well as imparting antimicrobial and antistatic properties to them to produce a novel silver nanoparticle–wool composite material. This is accomplished by the reduction of silver ions in solution by trisodium citrate (TSC) in the presence of merino wool fibers or fabrics. The silver metal nanoparticles simultaneously bind to the amino acids of the keratin protein in the wool fibers using TSC as the linker. The colors of the resulting merino wool–silver nanoparticle composites range from yellow/brown to red/brown and then to brown/black, because of the surface plasmon resonance effect of silver, and are tuned by controlling the reduction of silver ions to silver nanoparticles to give the required particle size on the fiber surface. In addition to the surface plasmon resonance optical effects, the silver nanoparticle–wool composites exhibit effective antimicrobial activity, thus inhibiting the growth of microbes and also an increase in the electrical conductivity, imparting antistatic properties to the fibers. Therefore, silver nanoparticles function as a simultaneous colorant and antimicrobial and antistatic agent for wool. Chemical and physical characterizations of the silver nanoparticle–merino wool composite materials have been carried out using scanning electron microscopy, transmission electron microscopy, energy-dispersive spectroscopy, synchrotron radiation X-ray diffraction, atomic absorption spectroscopy, X-ray photoelectron spectroscopy, direct-current electrical conductivity measurements, wash-fast and rub-fast tests, and antimicrobial tests.

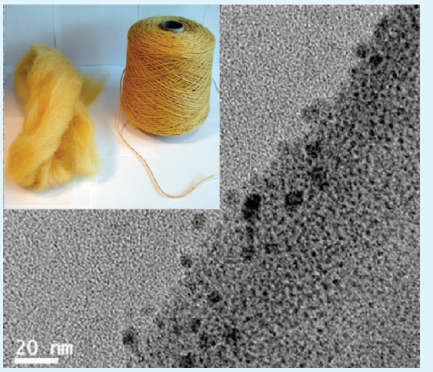

KEYWORDS: silver nanoparticles, colorant, wool, surface plasmon resonance, antimicrobial, antistatic

INTRODUCTION

This paper presents the formation and characterization of new silver nanoparticle–wool fiber composites, which are colored by the surface plasmon resonances of the silver nanoparticles and also exhibit effective antimicrobial and antistatic properties because of the silver. For this, a simple one-step preparation method is described, whereby Ag^+ is reduced to Ag^0 by trisodium citrate (TSC) in the presence of merino wool fibers with simultaneous binding of the nanoparticles to the merino wool fiber surface utilizing excess TCS as a linker to amino acids of the keratin protein. To our knowledge, this is the first time silver nanoparticles have been used as novel colorants for wool fibers while at the same time imparting antimicrobial and antistatic properties to them.

Merino wool is a natural protein fiber with diameters typically in the 12–20 μm range. It belongs to a group of fibrous proteins consisting of keratin, a helix-shaped protein molecule among a complex mixture of proteins with an irregular structure. Silver and silver-based compounds are historically known for their antimicrobial properties, showing strong biocidal effects[1] on as many as 650 species of microbes including *Escherichia coli*,[2,3] *Staphylococcus aureus*,[4,5] and HIV-I.[6] Silver species have been used as antimicrobial agents on cotton, silk, and synthetic textiles.[5,7−11] Methods for their preparation include silver plating of polyester/cotton blends,[10] radio-frequency plasma, and vacuum-ultraviolet surface activation of polyester–polyamide followed by chemical reduction of silver salts,[12] and layer-by-layer deposition of preformed silver nanoparticles onto nylon or silk.[5]

We have previously reported on merino fiber–conducting polymer–silver composites, whereby the redox-active polypyrrole or polyaniline polymer surface has reduced Ag^+ to Ag^0 nanocrystals, depositing them on the surface of the conducting polymer composite and imparting the antimicrobial nature of silver.[13]

When the particle size of silver is reduced to nanoscale dimensions, the antimicrobial and electrical properties remain, yet the conventional metallic color of silver is no longer observed. Instead, silver nanoparticles exhibit a variety of brilliant hues because of strong visible absorptions, which arise from the coherent oscillation of conduction band electrons from the resonance interaction with the electromagnetic field of visible light, known as surface plasmon resonance and theoretically explained by Mie theory in 1908.[14] The color observed is dependent on the size and shape of the nanoparticles.[15] Also, because of their large specific surface area, silver nanoparticles exhibit increased chemical and microbial activity[16] compared with the bulk form.

By harnessing the surface plasmon resonance effects of silver nanoparticles to provide a range of colors as well as their enhanced inhibitory action against microbes, we have captured a unique opportunity to provide a nanotechnology to develop

Received: December 12, 2010
Accepted: March 7, 2011
Published: March 07, 2011

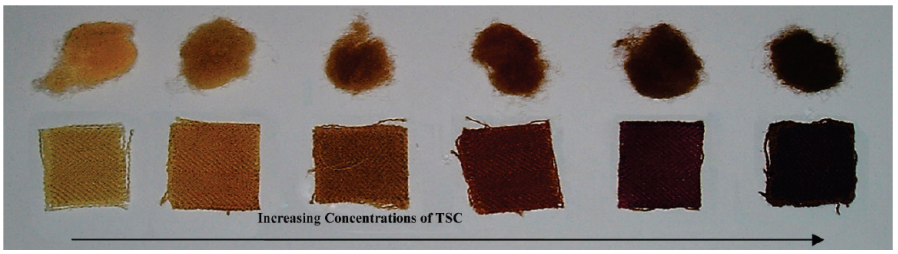

Figure 1. Merino wool fibers and fabric colored by silver nanoparticles prepared with different amounts of TSC, showing the effect of increasing TSC on the color.

new functional merino wool textiles for fashion apparel, interior furnishings, and carpets that comprise only wool and silver.

EXPERIMENTAL SECTION

Preparation of Silver Nanoparticle−Wool Composites. 100% merino wool yarns with a fiber diameter of about 19 μm provided by Ashford Handicrafts, Ashburton, New Zealand, were used. The merino fabric was provided by AgResearch, Christchurch, New Zealand. The preparation of silver nanoparticle−merino wool composites was accomplished by the reduction of silver ions to elemental silver, Ag^+ to Ag^0, from solution directly onto the fiber surface. Merino wool fibers (0.05 g) were heated in silver nitrate ($AgNO_3$; 10 mL, 250 or 500 mg kg^{-1}) until a constant temperature of 95 °C was obtained. When 95 °C was reached, varying quantities of trisodium citrate (TSC; 10, 20, and 50 μL each of 1% w/w or 10% w/w) were added as the reducing agent. Over a period of 10 min, silver nanoparticles of varying sizes and, hence, colors were generated and simultaneously bound to the surface of the fibers (Figure 1). The resulting composite fibers were washed thoroughly with distilled water and subjected to sonication to remove any unbound nanoparticles.

Silver nanoparticles prepared in a solution phase are predisposed to reduce surface tension by aggregation, and it is usually necessary to protect against this by using surfactants or polymeric ligands. However, such a protecting agent is not required for the method presented here because the TSC used in the reduction step acts as a linker to immediately bind the silver nanoparticles to the wool fibers and consequently stabilize them. In this way, the effective particle size of the nanosilver entities and hence the color are retained, thereby providing a novel colorant for the wool fibers, which are durable to repeated washing and rubbing.

Characterization of Silver Nanoparticle−Wool Composites. Silver nanoparticle−merino wool composites were characterized with respect to their color properties by measurements of their CIE L^*, a^*, b^*, and 457 nm brightness values using a HunterLab ColorQuest spectrophotometer, fitted with a Daylight 65 lamp. The composite fibers were stretched across the light source, and the light trap was placed behind so the measurements taken were for the composite only. The L^* value gives the degree of brightness (100 = white; 0 = black). The a^* value gives the sample's color tone between red (+ve) and green (−ve). The b^* value gives the color tone between yellow (+ve) and blue (−ve).

The morphology and composition of the silver nanoparticle−merino wool composites were examined by scanning electron microscopy (SEM) using a JEOL 6500 F field-emission scanning electron microscope equipped with an energy-dispersive spectroscopy (EDS) analysis system. Individual fibers were mounted on aluminum specimen stubs with double-sided carbon adhesive tape and sputter-coated, first with a platinum layer and then carbon, to provide a conductive layer in order to reduce the buildup of charges on the surface of the sample. The samples were viewed at sequential magnifications under secondary electron and backscatter conditions.

Transmission electron microscopy (TEM) analyses of silver nanoparticle−merino wool composites were performed on a JEOL 2011 high-resolution instrument with a LaB_6 filament operated at 200 kV. Because of the organic nature of merino wool, the composites first required dehydration and embedding in resin with a 54:32:12:1 Procure 812/NMA/DDSA/BDMA composition from which thin slices were cut for TEM analysis.

The quantification of the uptake of silver onto the fiber surface was carried out by measuring the amount of residual silver in the nanoparticle-forming solution by atomic absorption spectroscopy (AAS) using a GBC 906AA spectrometer. Because the nanosilver content was too low to provide an X-ray diffraction (XRD) pattern using a conventional instrument, XRD patterns of silver nanoparticle−merino wool composites were obtained on the powder diffraction beamline at the Australian Synchrotron, Melbourne, Australia. Data were collected in transmission mode with a beam size of 5 mm (horizontal) × 2 mm (vertical) and wavelength of 1.0003 Å. Sample preparation involved sandwiching of the silver nanoparticle−merino wool composite fibers between two sample holder plates with a circular hole of 15 mm diameter in the center.

X-ray photoelectron spectroscopy (XPS) was used to study the chemical bonding between the fiber substrate and the silver nanoparticulate coating through the respective binding energies of the core electrons. Measurements were carried out using a Kratos XSAM800 photoelectron spectrometer at the University of Auckland, Auckland, New Zealand. The spectra were collected using Al Kα radiation, with the energy scale being calibrated to the C 1s peak at 285.0 eV. The sample area measured was 300 × 700 μm. The electrical conductivity of the silver nanoparticle−merino wool composites was investigated by taking direct-current conductivity measurements of single fibers using a linear four-point probe method.

The colorfastness of the silver nanoparticle−merino wool composites to washing was tested at AgResearch, Christchurch, New Zealand, using the Australian/New Zealand Standard 2111.19.2 test. This test was carried out at 40 °C using a shampoo comprising sodium dodecylbenzenesulfonate (1 g dm^{-3}) and lauric monoisopropanolamide (0.2 g dm^{-3}) at pH 7.5. The performance is expressed on a scale of 1−5, where 1 indicates very poor colorfastness (maximum color change) and 5 indicates very high colorfastness (minimum color change). According to Australian/New Zealand Standard, the pass level for a change in the shade of color is 4. Also, a simulated washability test was carried out by placing the silver nanoparticle−merino wool composites in a H_2O/detergent solution (200:1) using a commercial washing powder (Persil) at 40 °C and agitating for a period of 24 h. This is equivalent to about 50 washes. The color change over time was measured by changes in the CIE L^*, a^*, and b^* values. The colorfastness of the silver nanoparticle−merino wool composites to rubbing in both wet and dry conditions was also carried out at AgResearch, Christchurch, New Zealand, according to the Australian/New Zealand Standard 2111.19.1. The performance is similarly evaluated on a relative scale of 1−5, where a pass requires a minimum value of 3 or 4 for dry rubbing and a minimum of 3 for wet rubbing.

Antimicrobial testing of the silver nanoparticle−merino wool composites was performed at the PTA Microbiology Laboratory of Capital and Coast Health, Wellington Hospital. Samples were placed on agar plates previously inoculated with a bacterial suspension of the pathogen *S. aureus* (ATCC 25923) and incubated for 24 h to allow for bacterial growth. All samples were tested against reference samples of untreated merino wool fibers, merino wool fibers treated with TSC only, and a silver wire. The extent of the zone of inhibition of bacteria around the sample was taken as a relative measure of the antimicrobial effectiveness of the composite.

RESULTS AND DISCUSSION

Physical Characterization and Morphology. *Color.* Figure 1 shows samples of merino wool and fabric colored by silver nanoparticles of different particle sizes and, hence, colors. By an increase in the amount (volume and concentration) of TSC as the reducing agent for the reduction of Ag^+ to Ag^0, the resulting silver nanoparticle−merino wool composites changed in color from yellow/orange to red/brown to brown/black. The CIE L^*, a^*, and b^* values, quantitatively characterizing the observed color of these samples, are given in Table 1. The original merino wool and fabric were a white/cream color, as shown by a high L^* value (whiteness), a small b^* value (a slight yellow undertone), and essentially zero b^* value (red/green undertone). Soaking the wool or fabric in TSC had no effect on the color.

The color is due to the surface plasmon resonance effects of silver nanoparticles, with a progressive change in color resulting from an increase in the size of the silver nanoparticles as more Ag^0 is formed on the nanoparticle surface with increasing amounts of reductant. At low levels of the TSC reducing agent, the color is yellow/orange, as shown by the high b^* value and midrange L^* value due to the typical 430 nm surface plasmon absorption of nanosilver. As the amount of 1% w/w TSC is increased, the color takes on a much greater red tone and a slightly less yellow tone and becomes darker, as shown by the increase in a^*, the small decrease in b^*, and the decrease in L^*, respectively (Table 1). There is a marked change in the color when the concentration of TSC is increased to 10% w/w, where the b^* value is significantly lower while the a^* value remains relatively high because of the more red/brown color. With the highest amount of TSC used, a more brown/black color is produced, with the a^* value being close to zero, the b^* value showing a small blue tone, and the L^* value being low. The 457 nm brightness is essentially the reflectivity at this wavelength. It decreases with a decrease in whiteness, as is shown by the decreasing L^* values with increasing amounts of TSC reducing agent. Overall, the colors represent an attractive "autumn range" and hence show that the silver nanoparticles can be used to provide novel colorants for merino wool fibers.

The increase in the average size of the silver nanoparticles on the surface of merino wool fibers can be correlated with the observed color change from yellow/orange to red/brown to brown/black (Figure 1), thereby confirming the dependence of the wavelength of the reflected light on the particle size. The SEM and TEM images (Figures 2 and 3, respectively) show that with an increase in the amount of reducing agent (concentration and volume), larger discrete particles and more aggregates of small particles appear. Also, the TEM images show that, with increasing reducing agent, there is a much larger spread in the particle size.

The optical absorption spectra of noble metal nanoparticles are dominated by surface plasmon resonance effects. With an increase in the particle size, the absorption band is shifted to longer wavelengths. When nanoparticles are sufficiently close together, interactions between neighboring particles arise so that models for isolated particles do not hold.[17] Thus, the optical absorption of a particular size aggregate comprising smaller

Table 1. CIE L^*, a^*, and b^* Values and 457 nm Brightness of Merino Wools Colored by Silver Nanoparticles

sample	L^*	a^*	b^*	457 nm brightness
merino wool	75.2	−0.7	3.7	49.7
10 μL of 1% w/w TSC	54.9	1.47	17.1	14.9
20 μL of 1% w/w TSC	41.8	4.56	16.1	7.4
50 μL of 1% w/w TSC	32.2	6.19	14.9	6.0
10 μL of 10% w/w TSC	29.3	5.49	6.11	4.7
20 μL of 10% w/w TSC	25.8	3.57	6.44	3.6
50 μL of 10% w/w TSC	25.0	−0.37	3.98	3.2

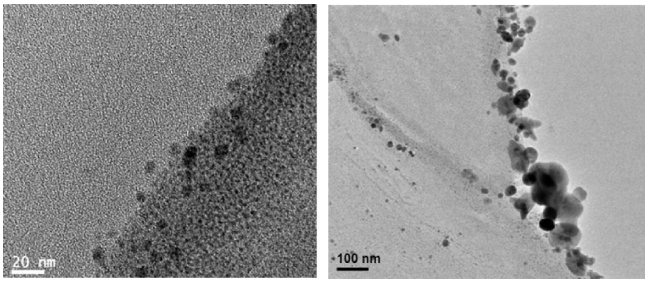

Figure 3. TEM images of a cross section of a silver nanoparticle−merino wool composite fiber prepared using (left) 20 μL of 1% w/w TSC and (right) 50 μL of 10% w/w TSC.

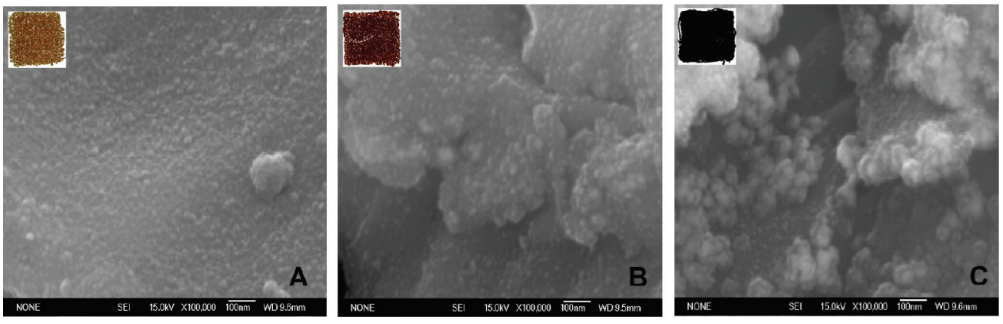

Figure 2. SEM images of silver nanoparticle−merino wool composites prepared with (A) 20 μL of 1% w/w TSC, (B) 10 μL of 10% w/w TSC, and (C) 50 μL of 10% w/w TSC. The scale bar depicts 100 nm.

particles will be similar to that of a single large nanoparticle comparable in size to the aggregate. The absorption is broadened and shifted and the color changes to a more dark-brown tone when a range of particle sizes is present, which occurs here with increasing levels of reducing agent. Metallic nanosilver has an intense plasmon absorption band in the visible region. It has been reported that the Ag 4d to 5sp interband transition generally occurs around an energy corresponding to 430 nm.[18] However, the surface plasmon resonance strongly depends on the dielectric function of the surrounding medium. The characteristic red shift of the plasmon absorption band observed in the spectra of the silver nanoparticle−merino wool composites is typical of silver nanoparticles protected by a stabilizing agent.[19]

The visible absorption spectra for silver nanoparticle−merino wool composites are shown in Figure 4. When 20 μL of 1% w/w TSC is used as the reducing agent, the composite is yellow/orange in color. The absorption spectrum of this sample shows a peak centered at ∼430 nm typical for silver nanoparticles of about 10 nm in size. Absorption is therefore in the blue end of the visible spectrum, and thus yellow/orange light is reflected, giving rise to the observed color. When 10 μL of 10% w/w TSC is used as the reducing agent, a further red shift in the plasmon band from ∼435 to ∼480 nm is observed. This shift produces a change in color from yellow/brown to more red/brown. The broad nature of the absorption band indicates that the sample contains both aggregated particles and a range of particles of a larger size. This is confirmed by SEM and TEM analysis (Figures 2 and 3). When 50 μL of 10% w/w TSC is used as the reducing agent, the resulting silver nanoparticle−merino wool composite is dark brown/black in color because the sample absorbs almost all colors in the visible region to the same extent (Figure 4).

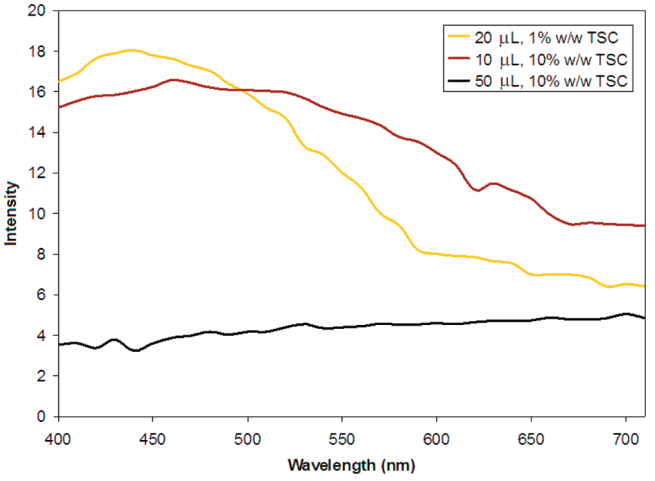

Figure 4. Visible absorption spectra for silver nanoparticle−merino wool composites prepared by with different amounts of TSC as the reducing agent: 20 μL of 1% w/w TSC; 10 μL of 10% w/w TSC; 50 μL of 10% w/w TSC.

SEM images of the silver nanoparticle−merino wool composites (Figure 2) show that the size and aggregation of the silver nanoparticles formed on and within the wool increase with increasing amounts (volume and concentration) of TSC, which correlates nicely with the change in color (Figure 1). An increase in the nanoparticle diameter from ∼15 nm (20 μL of 1% w/w TSC) to ∼20 nm (10 μL of 10% w/w TSC) to ∼50 nm (50 μL of 10% w/w TSC) is observed with a corresponding color change from yellow/orange to brown/black. The TEM results of the silver nanoparticle−merino wool composites prepared with 20 μL of 1% w/w TSC and 50 μL of 10% w/w TSC (Figure 3) similarly confirm the increase in the particle size as the volume and concentration of TSC increase. TEM provides more precise information on the sizes of individual silver nanoparticles. When 20 μL of 1% w/w TSC is used to reduce Ag^+ to Ag^0, the formed nanoparticles are ∼10 to ∼15 nm in size and are relatively homogeneous. However, when 50 μL of 10% w/w TSC is used, the nanoparticles formed vary quite considerably in size, from ∼10 up to ∼100 nm (Figure 3), giving the brown/black color due to absorption across a wider range of wavelengths in the

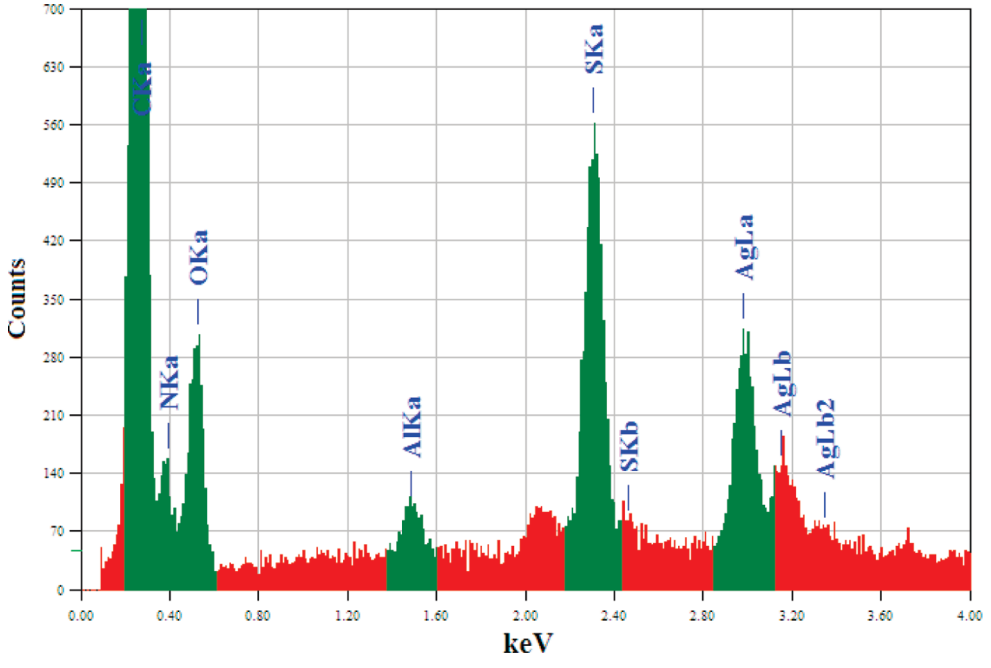

Figure 5. EDS elemental analysis spectrum of a silver nanoparticle−merino wool composite prepared with 50 μL of 10% w/w TSC.

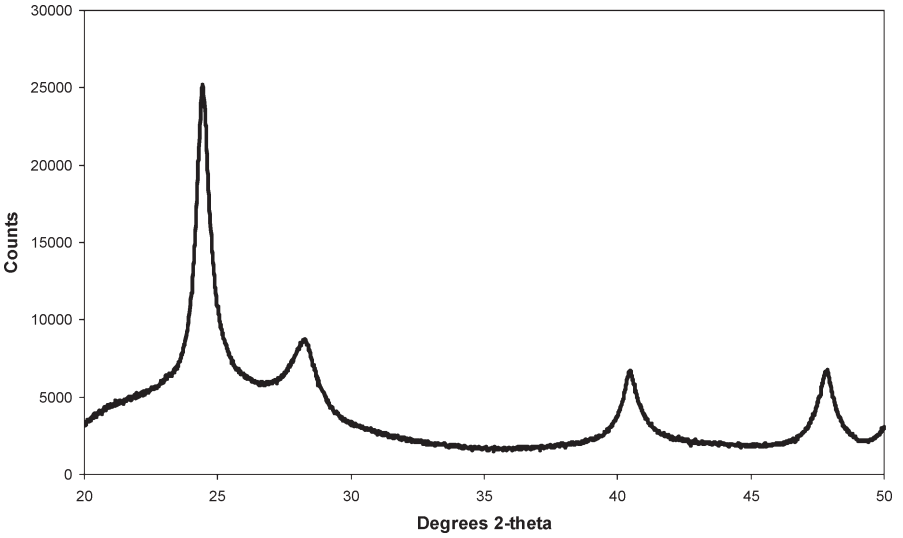

Figure 6. Synchrotron radiation XRD pattern of an untreated silver nanoparticle−merino wool composite prepared with 50 μL of 10% w/w TSC.

visible region. Again, this correlates well with the color, CIE values, and visible absorption spectra.

Confirmation of Silver Species. The presence of silver within the silver nanoparticle−merino wool composites was confirmed by elemental analysis with EDS, in addition to synchrotron radiation XRD, which shows metallic silver. SEM EDS elemental analysis of a silver nanoparticle−merino wool composite shows carbon, nitrogen, oxygen, and sulfur present in proteins that form the bulk of the wool fiber (Figure 5). The presence of silver within the silver nanoparticle−merino wool composite is confirmed by a peak at 2.98 keV corresponding to Ag Lα X-rays. Because the samples were prepared on aluminum stubs, this element is also detected. The synchrotron radiation XRD pattern for a silver nanoparticle−merino wool composite confirms that silver is present in its crystalline metallic form (Figure 6). The most intense peak, due to diffraction from the Ag(111) planes is centered at 24.4° 2θ. Peaks relating to diffraction from the Ag(200), Ag(220), and Ag(311) planes are observed at 28.3, 40.4, and 47.9° 2θ, respectively.

Extent of Silver Uptake by Merino Wool Fibers. The uptake of silver by merino wool during the preparation of silver nanoparticle−merino wool composites was quantified by AAS analysis. This was achieved by measuring the amount of residual silver in solution after the addition of TSC and binding the nanoparticles to the merino wool fibers. The results of the study show that an increase in the amount of the TSC reducing agent simultaneously increases the amount of silver ions removed from solution (Figure 7). At low amounts of reductant (10 μL of 1% w/w TSC), only partial conversion of Ag^+ to silver nanoparticles is observed, where ∼25% of Ag^+ in solution is removed as nanoparticles. However, at high concentrations of TSC (50 μL of 10% w/w TSC), a nearly complete conversion of Ag^+ (∼95%) to silver nanoparticles is observed. This yields a greater number of silver nanoparticles with a larger particle size and size range (Figure 3). The effect is the same for solutions containing 250 and 500 mg kg^{-1} Ag^+, which shows the importance of the amount of the TSC reducing agent in controlling the formation of silver nanoparticles on the wool fiber. The residual unreduced silver remains in solution and is not taken up by the wool fiber. As discussed later, XPS measurements show that the silver

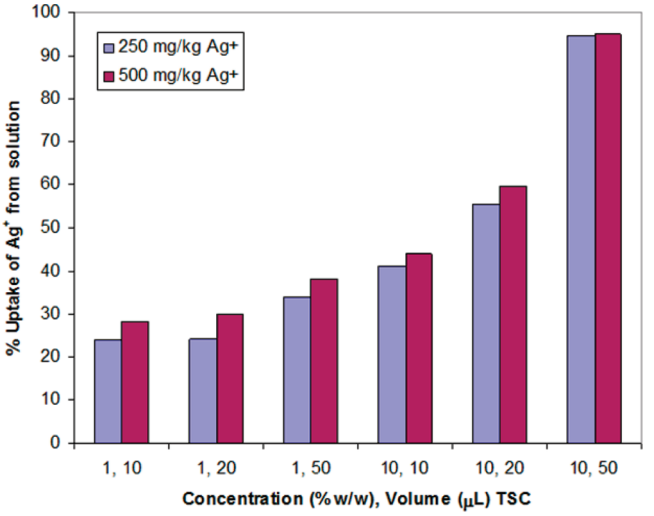

Figure 7. Percentage uptake of silver by merino wool fibers when reduced with increasing amounts of TSC.

nanoparticles chemically bind to TSC, which acts as a linker to bind the nanoparticles to the wool fiber.

The increase in metallic silver on the surface and within untreated merino wool fibers with an increase in TSC was further confirmed by synchrotron radiation XRD. When the amount of reducing agent used was increased, the peak relating to Ag(111) increased in intensity (Figure 8). These results support the argument that the color change of samples from yellow to yellow/orange and red/brown to blue/black is related to an increase in the amount and size of silver nanoparticles on the surface of merino wool.

Binding of Nanoparticles to Merino Fibers. The formation of silver nanoparticles using TSC as the reducing agent proceeds according to the following equation:

$$2Ag^+ + Na_3C_6H_5O_7 \rightarrow 2Ag^0 + Na_2C_5H_4O_5 + Na^+ + H^+ + CO_2$$

Immediately following the reduction, additional negatively charged citrate ions are adsorbed onto the silver nanoparticles, introducing a surface charge that essentially forms an electrical

double layer. Because the citrate-coated particles are negatively charged on the outside, they repel one another and prevent particle aggregation. In this respect, aggregation to form larger particles is only likely to occur during formation of the initial bilayer.

Keratin, the main constituent of wool fibers, has an abundance of molecular groups on its surface. In particular, amino acids containing nitrogen, sulfur, and carboxylate functional groups are prevalent, all of which have the potential to bind to silver nanoparticles.[20−22] In order to determine the mode of chemical bonding between the merino wool fiber substrate and the silver nanoparticles, XPS studies were carried out. Figure 9 presents XPS data for the Ag 3d electrons of silver nanoparticles and the silver nanoparticle−merino wool composite material. XPS O 1s, N 1s, and S 2p spectra of untreated merino wool and the silver nanoparticle−merino wool composite are presented in Figure 10. For ease of comparison, the vertical scale for some data has been expanded. As detailed below, these XPS studies show that TSC acts as both a stabilizer of the nanoparticles and a linker to either nitrogen- or sulfur-containing groups in the amino acids of proteins on the surface of the fiber, as shown in Figure 11.

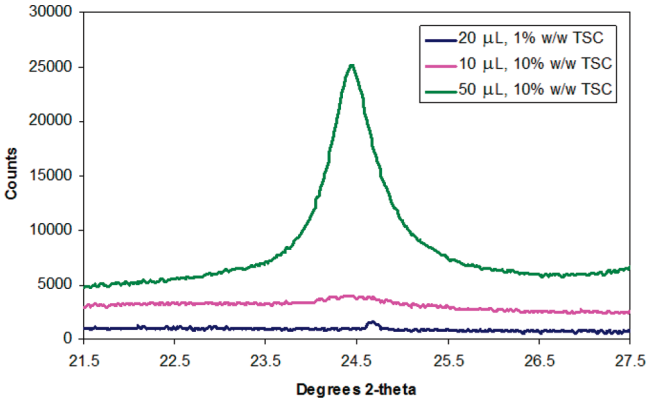

Figure 8. Synchrotron radiation XRD pattern showing the Ag(111) peak for a silver nanoparticle−merino wool composite, using different amounts of TSC as the reducing agent.

The experimental peak envelope of the Ag 3d spectrum (Figure 9, black curves) for silver nanoparticles prepared by the reduction of Ag^+ with TSC can be assigned to two components. The major component is Ag^0, due to the reduction of Ag^+ by TSC, and the lesser component is Ag−O−, due to positively charged silver ions on the surface of the nanoparticle being bound to the anionic oxygen of the carboxyl group of the citrate (Figure 9, red fitted curves). When the positions of these fitted peaks are compared with those for the comparable fitted peaks for the Ag 3d spectrum of the silver nanoparticle−merino wool composite (Figure 9, purple fitted curves), it is seen that there is a distinct shift to higher binding energies for peaks relating to Ag^0 (368.3−368.7 eV) and Ag−O− (369.3−370.1 eV) in the Ag 3d spectrum. Of significance, is the increased shift of the Ag−O− peak of the silver nanoparticle−merino wool composite. This indicates that the citrate ions stabilizing the silver nanoparticles are also bound to a second entity, which is the keratin protein in the wool fiber. This confirms a chemical interaction between the silver nanoparticles and the merino wool fiber through TSC as a linker.

This interaction of the carboxyl groups of the citrate surrounding the silver nanoparticles with the protein in the merino wool is further shown by the O 1s XPS spectra (Figure 10, top spectrum, blue curve). A single broad peak at 532.4 eV can be fitted to the experimental spectrum for the merino wool, reflecting an average of the different oxygen environments in the amino acids of the wool protein (Figure 10, top spectrum, blue curve). However, the experimental O 1s XPS spectrum for the silver nanoparticle−merino wool composite has a broad shoulder at about 534 eV, and this spectrum can be fitted to two component peaks (Figure 10, top spectrum, purple curves). The peak at ∼532 eV similarly represents the different oxygen environments in the amino acids of the wool protein. However, the shoulder peak at the higher binding energy of 534.1 eV can be assigned to a carboxyl group bound to an alternative species, which is TSC.

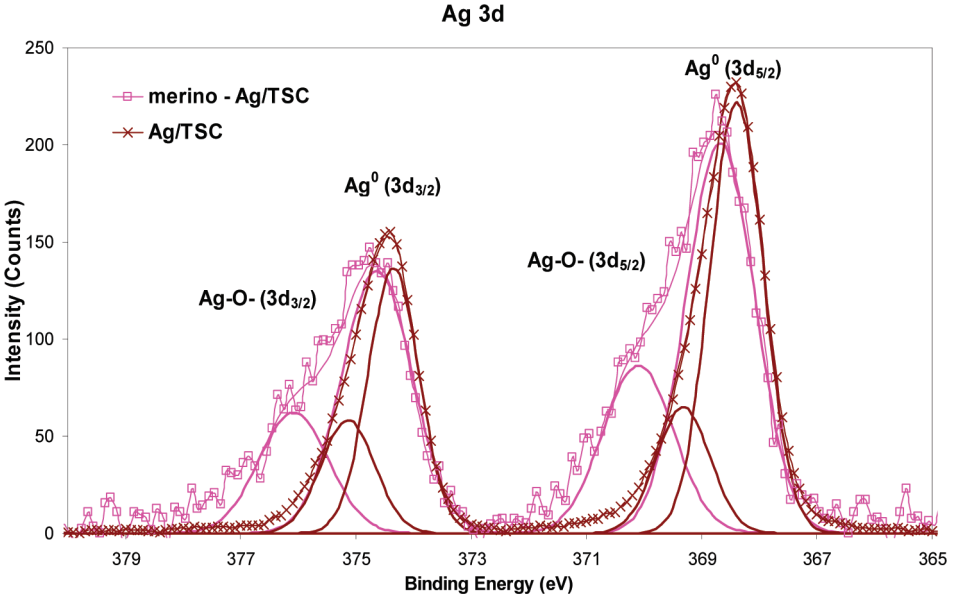

Figure 9. Superimposed experimental and fitted XPS spectra for Ag 3d electrons for silver nanoparticles (black fitted curves) and a silver nanoparticle−merino wool composite prepared with 50 μL of 10% w/w TSC (purple fitted curves).

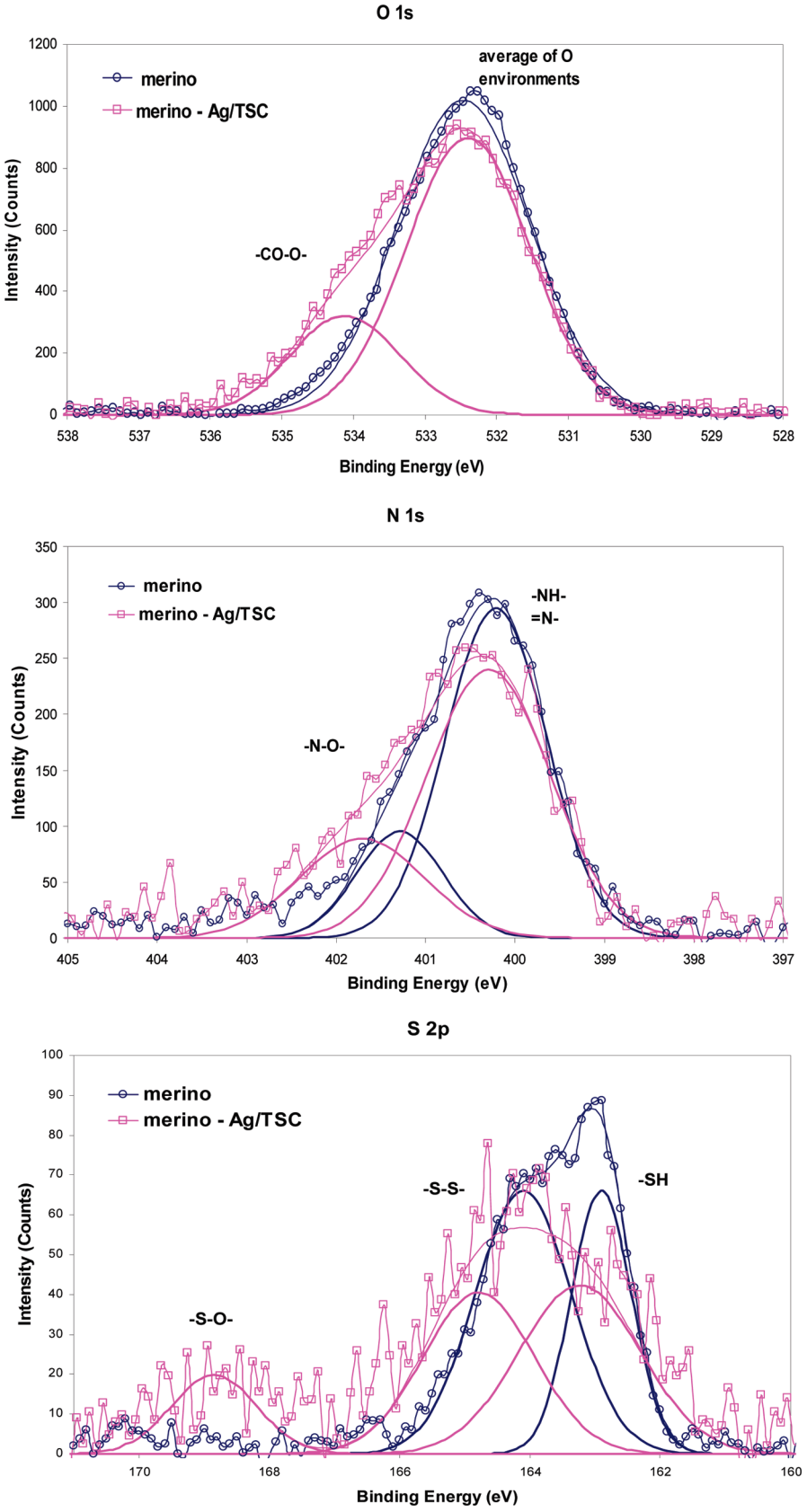

Figure 10. Superimposed experimental and fitted XPS spectra for untreated merino wool (black) and a silver nanoparticle−merino wool composite prepared with 50 μL of 10% w/w TSC: (top) O 1s electrons; (middle) N 1s electrons; (bottom) S 2p electrons.

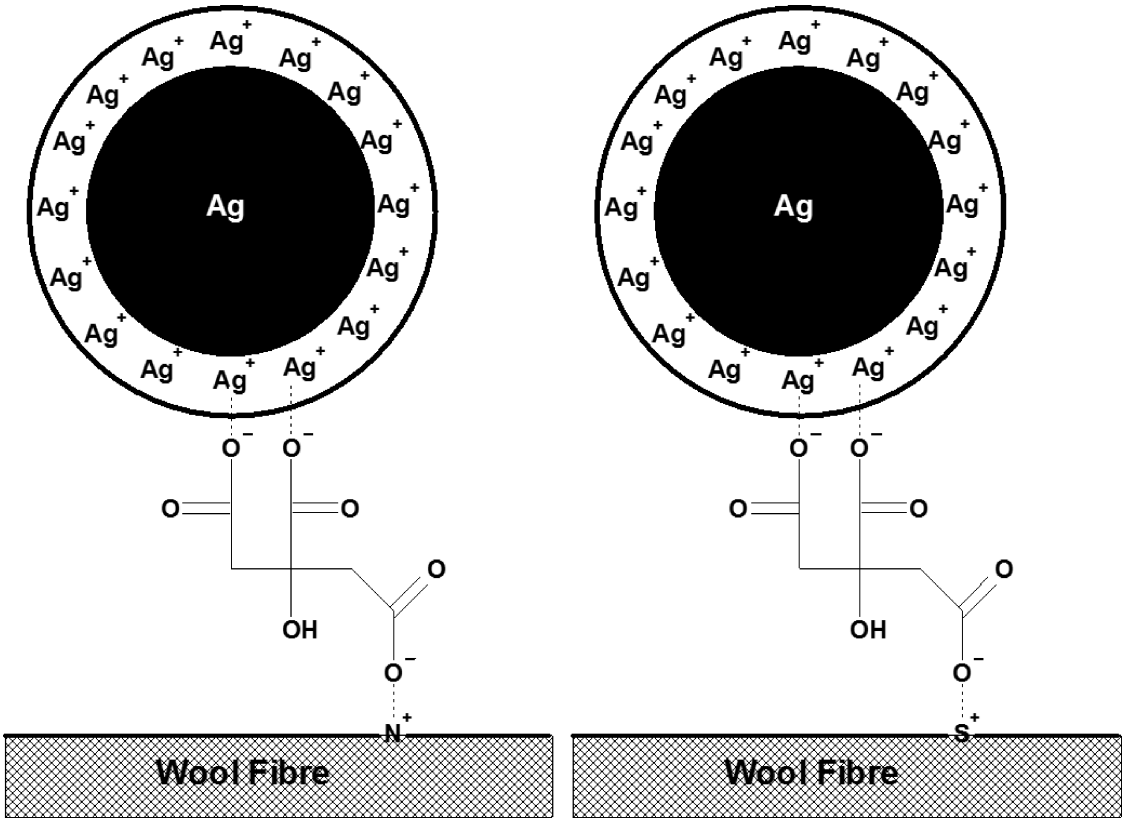

Figure 11. Schematic of the bonding of TSC to the surface of silver nanoparticles, whereby the citrate also acts as a linker to the amino acids in the keratin protein of the wool fiber.

The experimental XPS spectra of N 1s for the merino wool and the silver nanoparticle−merino wool composite (Figure 10, middle spectra, blue and purple curves) can each be fitted to two peaks representing amine/imine nitrogen and −N−O nitrogen. This shows the presence of some oxidized nitrogen in the base merino wool, which probably arises from the wool scouring and pretreatment processes that the wool has been subjected to prior to us receiving it. There is essentially no change in the binding energy of the peaks occurring at 400 eV for the amine/imine nitrogen between the merino wool and the silver nanoparticle−merino wool composite (Figure 10, middle spectra, blue and purple curves), showing that the amine/imine environments in both samples are very similar. Thus, it is assumed there is no change in the bonding environments of these groups in the amino acids in the composite wool. However, a significant shift in the peak assigned to −N−O nitrogen is observed from 401.2 to 401.7 eV (Figure 10, middle spectra, blue and purple curves), which is consistent with a chemical-bonding interaction between these nitrogen atoms in the proteins on the surface of the wool with the citrate. This further confirms the role of citrate as a linker in the binding of silver nanoparticles to amino acids in the wool.

The experimental XPS spectra for the S 2p spectra for the merino wool and the silver nanoparticle−merino wool composite (Figure 10, bottom spectra, blue and purple curves) are not as well-resolved and, hence, the fitted curves must be treated with caution and cannot be compared absolutely. Even so, it is possible to see that the $^{3}/_{2}$ and $^{1}/_{2}$ S 2p peaks occurring at 162.9 and 164.1 eV, respectively, in the base merino wool (Figure 10, bottom spectra, black fitted curves), which represent the average −S−H and −S−S− environments of the cystine amino acids, are shifted to higher binding energies by about 1 eV for the silver nanoparticle−merino wool composite (Figure 10, bottom spectra, pink fitted curves). This similarly confirms chemical interaction presumably with TSC of the silver nanoparticles and the sulfur in the cystine amino acids. It is further confirmed by the peak at 168.8 eV in the spectrum of the silver nanoparticle−merino wool composite, showing the presence of a small amount of −S−O− type sulfur and chemical bonding between the sulfur and TSC.

The XPS study of silver, oxygen, nitrogen, and sulfur therefore collectively shows the presence of chemical-bonding interactions between the silver nanoparticles and TSC and the sulfur and nitrogen of the amino acids in the wool fiber and TSC, confirming the role of TSC as a linker to chemically bind the silver nanoparticles to the wool fiber. This is shown diagrammatically in Figure 11.

The presence of this chemical linkage is important in ensuring the durability of the silver nanoparticle−merino wool composite toward rubbing and washing, which is a necessary requirement for their use in textile applications. This durability has been ably demonstrated by the favorable results from the washing and rubbing tests presented below.

Electrical Conductivity. Merino wool yarns themselves are not inherently electrically conducting ($<10^{-10}$ S cm^{-1}). At low concentrations of TSC and thus low concentrations of silver nanoparticles on the fiber surface, no apparent increase in the electrical conductivity was observed. However, at higher concentrations of TSC (and, hence, higher concentrations of silver nanoparticles on the fiber surface), electrical conductivities

Figure 12. Inhibition zones of *S. aureus* microbial growth for a silver nanoparticle−merino wool composite: (A) 20 μL of 1% w/w TSC; (B) 10 μL of 10% w/w TSC; (C) 50 μL of 10% w/w TSC.

ranging from 3.2×10^{-5} to 4.0×10^{-5} S cm^{-1} were measured. This increase in the electrical conductivity into the weak semiconducting region is indeed significant and is sufficient to dissipate static electricity. The silver nanoparticle−merino wool composite fibers, therefore, provide an additional functional benefit to wool fibers and have potential applications in antistatic textiles particularly in fabric seating upholstery and carpets.

Antimicrobial Testing. The silver nanoparticle−merino wool composite fibers actively inhibited the growth of *S. aureus* microbes. In Figure 12, the white, cloudy areas indicate bacterial growth, whereas transparent areas surrounding the silver nanoparticle−merino wool composites indicate bacterial-free regions, i.e., zones of inhibition. Higher concentrations of TSC used in the preparation of samples give increased zones of inhibition due to increased concentrations of nanoparticles on the surface of the fiber. For the reference samples, untreated merino wool fibers and merino fibers treated with TSC only showed no antimicrobial effects. The silver wire showed zones of inhibition of up to 3 times the diameter of the wire only, whereas the extent to which an individual silver-coated fiber can inhibit the growth of bacteria is up to approximately 100 times the diameter of the fiber. When considering the relative masses of silver present in the silver wire, in comparison to the silver nanoparticle−merino wool composites, the antimicrobial effect of the composites is even more significant. This is due to the higher specific surface area of the wool fibers and the nanosize of the silver entities, which collectively provide for the greater release of silver ions from the composite, which are the active antimicrobial species. These results show that the silver nanoparticle−merino wool composites exhibit effective antimicrobial properties.

Simulated Washability Testing. For the silver nanoparticle−merino wool composite fibers to be fabricated into useful textile and carpet products, it is important that the silver nanoparticles do not wash or wear off, as is the case in many nanosilver polymer composites. Spectrophotometric results, following the simulated washing of silver nanoparticle−merino wool composites in water/Persil detergent over 24 h, show that, after a very minimal initial

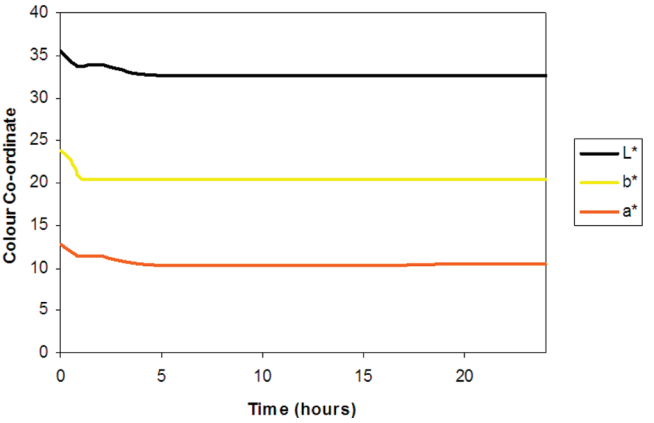

Figure 13. Change in the CIE L^*, a^*, and b^* optical values for a silver nanoparticle−merino wool composite with washing over a 24 h period.

shift in the color observed in the first hour of washing, the color remains stable for subsequent hours (Figure 13). The initial color change is likely due to loosely bound nanoparticles becoming dislodged from the fiber surface. Following this, the remaining silver nanoparticles, which are chemically bound to the surface through TSC as discussed above, are integral with the wool protein and provide a robust composite fiber. This provides a significant functional performance advantage. The colorfastness of the silver nanoparticle−merino wool composites to washing tested against the Australian/New Zealand Standard 2111.19.2 gave a result of 5, which is at the maximum end of the scale and above the pass level of 4. Similarly, the colorfastness of the silver nanoparticle−merino wool composites to rubbing in both wet and dry conditions tested against the Australian/New Zealand Standard 2111.19.1 gave a value of 4 or 5, which is above the pass level. Collectively, these results successfully demonstrate the durability of the silver nanoparticle−merino wool composites to washing and rubbing, which is a necessary requirement for their use in textiles.

CONCLUSIONS

Silver nanoparticles have been successfully synthesized and chemically bound to merino wool fibers to provide novel colorants through surface plasmon resonance effects as well as functional antimicrobial and antistatic properties. SEM and TEM studies of the silver nanoparticle−merino wool composite fibers show that the range of colors is controlled by the size and concentration of the nanoparticles. In the synthesis process, TSC first reduces Ag^+ to Ag^0 and then subsequently acts as a linker to bind nanoparticles to nitrogen- and sulfur-containing groups in the keratin protein on the merino wool surface. This was confirmed by XPS studies. As the proportion of silver nanoparticles on the fiber surface increases, adequate electrical contact between particles is permitted, and the electrical conductivity of the silver nanoparticles is transferred, imparting antistatic properties to the textiles. The colors obtained for the silver nanoparticle−merino wool composites are colorfast, as determined by simulated washability tests. The silver nanoparticles also impart antimicrobial properties to the fibers where their effectiveness against *S. aureus* microbes was successfully demonstrated. This method of preparation for the silver nanoparticle−merino wool composites, therefore, provides industry with a novel high-quality, high-value functional fiber for fashion apparel, textiles for furnishing applications, and carpets.

AUTHOR INFORMATION

Corresponding Author
*E-mail: jim.johnston@vuw.ac.nz.

ACKNOWLEDGMENT

Funding support from the NZTEC Bright Futures Top Achiever Doctoral Scholarship, the Polymer Electronic Research Centre (PERC), The University of Auckland, The MacDiarmid Institute for Advanced Materials and Nanotechnology, and the Curtis−Gordon Research Scholarship is gratefully acknowledged.

REFERENCES

(1) Liau, S. Y.; Read, D. C.; Pugh, W. J.; Furr, J. R.; Russell, A. D. *Lett. Appl. Microbiol.* **1997**, *25*, 279–283.
(2) Sondi, I.; Salopek-Sondi, B. *J. Colloid Interface Sci.* **2004**, *275*, 177–182.
(3) Kim, S.; Kim, H.-J. *Int. Biodeterior. Biodegrad.* **2006**, *57*, 155–162.
(4) Hamilton-Miller, J. M. T.; Shah, S. *Int. J. Antimicrob. Agents* **1996**, *7*, 97–99.
(5) Dubas, S. T.; Kumlangdudsana, P.; Potiyaraj, P. *Colloids Surf., A* **2006**, *289*, 105–109.
(6) Elechiguerra, J. L.; Burt, J. L.; Morones, J. R.; Camacho-Bragado, A.; Gao, X.; Lara, H. H.; Yacaman, M. J. *J. Nanobiotechnol.* **2005**, *3* (6), 1–10.
(7) Lee, H. J.; Yeo, S. Y.; Jeong, S. H. *J. Mater. Sci.* **2003**, *38*, 2199–2204.
(8) Bender, W.; Stutte, P. *ACS Symp. Ser.* **2001**, *792*, 218–242.
(9) Hipler, U.-C.; Elsner, P.; Fluhr, J. W. *Curr. Problems Dermatol.* **2006**, *33*, 165–178.
(10) Jiang, S. Q.; Newton, E.; Yuen, C. W. M.; Kan, C. W. *J. Appl. Polym. Sci.* **2006**, *100*, 4383–4387.
(11) Yuranova, T.; Rincon, A. G.; Pulgarin, C.; Laub, D.; Xantopoulos, N.; Mathieu, H. J.; Kiwi, J. *J. Photochem. Photobiol., A* **2006**, *181*, 363–369.
(12) Yuranova, T.; Rincon, A. G.; Bozzi, A.; Parra, S.; Pulgarin, C.; Albers, P.; Kiwi, J. *J. Photochem. Photobiol., A* **2003**, *161*, 27–34.
(13) Kelly, F. M.; Johnston, J. H.; Borrmann, T.; Richardson, M. J. *J. Nanosci. Nanotechnol.* **2008**, *8*, 1965–1972.
(14) Feldheim, D. L., Foss, C. A., Eds. *Metal Nanoparticles: Synthesis, Characterization, and Applications*; Marcel Dekker: New York, 2002.
(15) Mock, J. J.; Barbic, M.; Smith, D. R.; Schultz, D. A.; Schultz, S. *J. Chem. Phys.* **2002**, *116*, 6755–6759.
(16) Morones, J. R.; Elechiguerra, J. L.; Camacho, A.; Holt, K.; Kouri, J. B.; Ramirez, J. T.; Yacaman, M. J. *Nanotechnology* **2005**, *16*, 2346–2353.
(17) Wiley, B.; Sun, Y.; Mayers, B.; Xia, Y. *Chem.—Eur. J.* **2005**, *11*, 454–463.
(18) Henglein, A. *J. Phys. Chem.* **1993**, *97*, 5457–5471.
(19) Manna, A.; Imae, T.; Iida, M.; Hisamatsu, N. *Langmuir* **2001**, *17*, 6000–6004.
(20) Brack, N.; Lamb, R.; Pham, D.; Turner, P. *Surf. Interface Anal.* **1996**, *24*, 704–710.
(21) Bradley, R. H.; Mathieson, I.; Byrne, K. M. *J. Mater. Chem.* **1997**, *7*, 2477–2482.
(22) Bhadani, S. N.; Kumari, M.; Sen Gupta, S. K.; Sahu, G. C. *J. Appl. Polym. Sci.* **1997**, *64*, 1073–1077.